Surface Dose in the Treatment of Breast Cancer with Helical Tomotherapy

Felix Zibold, Florian Sterzing, Gabriele Sroka-Perez, Kai Schubert, Katja Wagenknecht, Gerald Major, Jürgen Debus, Klaus Herfarth[1]

Purpose: Investigation of the effects of breathing motion- and misregistration-induced errors on the superficial dose in the treatment of breast cancer using helical tomotherapy (HT).

Material and Methods: Surface dose measurements were performed with thermoluminescence dosimetry (TLD). Two treatment plans with different planning target volume (PTV) definitions of the left breast were used: PTV_{skin} had its ventral border exactly on skin level, while PTV_{air} included also a 10-mm extension ventral to the PTV_{skin}. With a thoracic static phantom, misregistration errors in an HT were simulated. A dynamic phantom was used to simulate a breathing patient during HT. Surface doses of breast cancer patients were measured both for an HT (179 points) and a conventional three-dimensional conformal treatment (70 points).

Results: In the static phantom misregistration setup, dose deviations of –31.9% for PTV_{skin} to +35.4% for PTV_{air} could be observed. The dynamic phantom measurements resulted in surface dose deviations from those in a static position between 0.8% and 3.8% without a significant difference for the PTV definitions. The measured surface doses on patients averaged (mean ± standard deviation) 1.65 ± 0.13 Gy for the HT and 1.42 ± 0.11 Gy for the three-dimensional conformal treatment.

Conclusion: HT enables a homogeneous and reproducible surface dose with small dose deviations in the treatment of breast cancer. HT is a feasible method to treat breast cancer under free shallow breathing of the patient using a treatment plan with a ventral PTV border on the skin level.

Key Words: Tomotherapy · Surface dose · Breast cancer · Breathing motion · TLD

Strahlenther Onkol 2009;185:574–81
DOI 10.1007/s00066-009-1979-7

Oberflächendosis in der Behandlung des Mammakarzinoms mit helikaler Tomotherapie

Ziel: Untersuchung der Effekte von atembewegungs- und fehlpositionierungsbedingten Störungen auf die Oberflächendosis in der Behandlung des Mammakarzinoms mit helikaler Tomotherapie (HT).

Material und Methodik: Die Oberflächendosismessungen wurden mit Thermolumineszenzdosimetrie (TLD) durchgeführt. Zwei Bestrahlungspläne mit verschiedenen Planungszielvolumen-(PTV-)Definitionen der linken Brust wurden verwendet: PTV_{skin} hatte seine ventrale Begrenzung exakt auf Hautniveau, während PTV_{air} zusätzlich eine 10-mm-Erweiterung ventral von PTV_{skin} enthielt. Mit einem statischen Thoraxphantom wurden verschiedene Fehlpositionierungen während einer HT simuliert. Ein dynamisches Phantom wurde verwendet, um eine atmende Patientin während einer HT zu simulieren. Die Oberflächendosen von Mammakarzinompatientinnen wurden sowohl bei HT (179 Messpunkte) als auch bei der dreidimensionalen konformalen Radiotherapie (70 Messpunkte) gemessen.

Ergebnisse: Im Versuch des statischen Phantoms konnten Dosisunterschiede von –31,9% bei PTV_{skin} bis +35,4% bei PTV_{air} beobachtet werden. Die Messungen mit dem dynamischen Phantom ergaben Dosisunterschiede von den Dosen in statischer Position zwischen 0,8% und 3,8% ohne einen signifikanten Unterschied zwischen den PTV-Definitionen. Die gemessenen Oberflächendosen von Patientinnen lagen durchschnittlich bei (Mittelwert ± Standardabweichung) 1,65 ± 0,13 Gy bei HT und 1,42 ± 0,11 Gy bei der dreidimensionalen konformalen Behandlung.

Schlussfolgerung: HT ermöglicht eine homogene und reproduzierbare Oberflächendosis mit geringen Abweichungen in der Behandlung des Mammakarzinoms. Die HT eignet sich zur Behandlung des Mammakarzinoms unter freier flacher Atmung der Patientin, wenn ein Bestrahlungsplan mit ventraler PTV-Begrenzung auf Hautniveau verwendet wird.

Schlüsselwörter: Tomotherapie · Oberflächendosis · Mammakarzinom · Atembewegung · TLD

[1]Department of Radiation Oncology, University of Heidelberg, Germany.

Received: December 3, 2008; accepted: May 11, 2009

Introduction

Helical tomotherapy (HT) is a form of intensity-modulated radiation therapy (IMRT), in which a 6-MV linear accelerator is installed on a ring gantry and rotates around the patient during treatment in a helical way, while the patient is constantly moved through the gantry bore [9, 10, 23]. This setup allows HT to combine a megavoltage computed tomography scanner (MV-CT) with a therapeutic linear accelerator in a single machine [2, 16, 17]. With HT a highly conformal dose distribution and precise positioning of the patient can be achieved [1, 4, 15, 18]. In the case of breast cancer treatment, the target volume extends up to the air-to-skin transition and is moved due to breathing motion. The combination of the high doses on the upper planning target volume (PTV) region and the constant motion of this area due to breathing make surface doses difficult to calculate and predict in HT [5, 24]. For three-dimensional conformal radiotherapy (3D-CRT), these issues are less problematic, because the two radiation fields can be opened up wider, so the area above skin level also belongs to the radiation field. The variations of the surface dose should be further investigated, since IMRT has proven to be a good method of radiation therapy after breast-conserving surgery especially for patients with funnel chest, parasternal tumor location and bilateral breast cancer [19–21].

The purpose of this study was to quantify the surface dose of a breast cancer treatment with HT under free breathing conditions. Furthermore, this study should give evidence about possible dose gradients in the air layer above the target region where the surface moves in and out due to breathing motion in different kinds of treatment plans. For these reasons, a static and a dynamic phantom setup were used to quantify dose gradients in the air layer above skin level and dose differences between radiation in static and dynamic conditions. The data of the phantom experiments was compared to surface dose measurements on patients in clinical routine. In each setup, a comparison between surface doses displayed in the planning software and measured doses was done, although other studies found, that the validity of the plan doses is limited near the air-to-skin transition [13]. Since the latest research has shown that the longitudinal breathing motion-induced dose error in the treatment of breast cancer with HT is relatively insignificant for typical breathing patterns, this study investigates the possible dose effects of motion in a transverse plane in the radiation field [8].

Material and Methods

Surface Dose Measurements and Statistics

Surface dose measurements were performed with 3.1 × 3.1 × 1 mm lithium fluoride thermoluminescence dosimetry (TLD) chips (PTW, Freiburg, Germany). The analysis of the TLD chips was done with a TOLEDO 654 TLD-Reader (Pitman Instruments, Weybridge, UK) while regeneration was performed with a PTW-TLDO oven (PTW). For the static phantom and patient measurements, plastic envelopes containing a TLD chip were taped on the surface, while the dynamic phantom had 1 mm deep holes to integrate single TLD chips. The TLD chips were calibrated via batch calibration with a measurement uncertainty of maximum 5% [14]. The Wilcoxon U-test was used as a two-tailed test to show differences between the measured surface doses of different treatment methods.

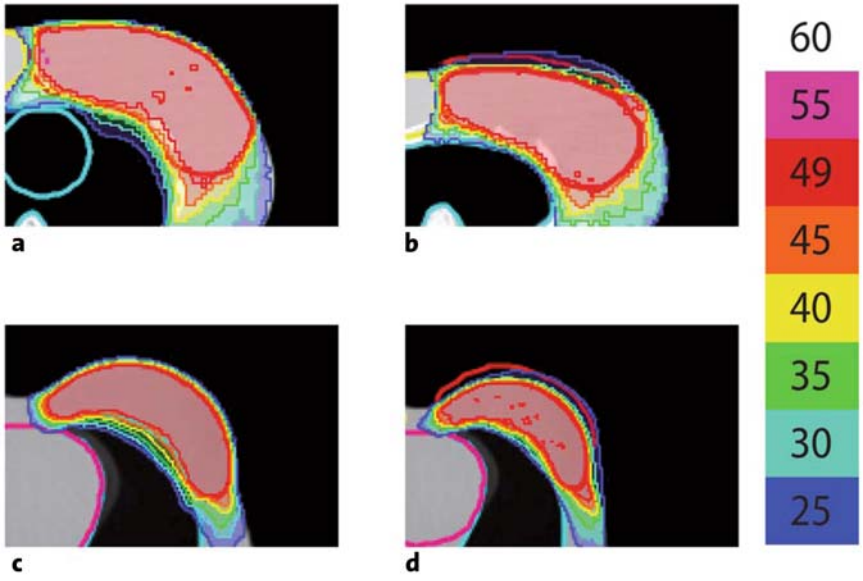

Figures 1a to 1d. Tomotherapy treatment plans used for the phantom measurements. Plans of the static phantom with PTV_{skin} (a) and PTV_{air} (b). Plans of the dynamic phantom with PTV_{skin} (c) and PTV_{air} (d). Corresponding isodose scale (right).

Abbildungen 1a bis 1d. Tomotherapiebestrahlungspläne der Phantommessungen. Pläne des statischen Phantoms mit PTV_{skin} (a) und PTV_{air} (b). Pläne des dynamischen Phantoms mit PTV_{skin} (c) und PTV_{air} (d). Dazugehörige Isodosenskala (rechts).

Treatment Planning

For treatment planning of the phantoms, the lung, the presumed area of the heart, the contralateral (right) breast and two different PTVs were segmented: PTV_{skin} included the left breast, the thoracic wall, and the superficial skin. PTV_{air} also included a PTV extension of 10 mm ventrally and left laterally "into the air" (Figure 1). TomoTherapy® planning software (Planning Station version 2.2.1.55; TomoTherapy® Inc., Madison, WI, USA) was used for treatment planning. Plan-

ning parameters included a field width of 2.5 cm, a pitch of 0.287, and a modulation factor of 4.0 [7]. The prescribed dose per fraction was 1.8 Gy, similar to the dose of a normal breast cancer treatment. Planning CTs were performed using a Siemens Somatom® (Siemens, Erlangen, Germany) and were driven as spiral CTs without motion of the phantoms to avoid another variable in the planning process, which was not directly issue of this study. The treatment plans of the patients corresponded to the plan PTV_{skin}. Treatment was performed on a TomoTherapy® treatment unit (TomoTherapy® Inc.). The three-dimensional conformal treatment was performed with a conventional plan made with HELAX 3D® (MDS Inc., Toronto, Canada) software with two tangential radiation fields on a Siemens Primus® linear accelerator (Siemens). Treatment plans for PTV_{skin} and PTV_{air} were first delivered on the static and dynamic phantom on normal planning position under static conditions and the mean value of the measurements was calculated as baseline for the following experiments.

Static Phantom

A static anthropomorphic thoracic phantom consisting of PMMA (Polymethylmethacrylat) (3M corp., St. Paul, MN, USA) was used for the static experiments (Figure 2). The surface dose was measured as the average of three spots in the PTV region. This setup should concentrate on the dose effects of a mispositioning in the anterior-posterior and lateral directions in the transverse plane of breathing motion to give possible evidence about the dose gradients being in this area in different types of plans in HT. Therefore, the phantom was positioned left and anterior of the normal position and afterwards right and posterior with a variation of 2/2, 5/5, 8/8, and 10/10 mm from normal position in each direction. For each variation, the PTV_{skin} and the PTV_{air} treatment plans were delivered on the phantom and the surface doses were measured. Figure 3 shows the dose gradients in an HT treatment plan of a typical breast cancer patient.

Dynamic Phantom

This setup should simulate the breathing motion in a transverse plane. As an enhancement of the static phantom setup, it should further investigate the dose effects of motion in the area of the dose gradient (measured in the static phantom setup). Therefore, a special dynamic phantom was constructed for the experiments: The phantom body was designed with original CT scans of a female patient using the anatomic information of surface, lungs, and heart (Figure 4). The body and the organs were reconstructed in eleven slices 10 mm thick with different artificial materials of the same physical density as the corresponding tissue. By installing the phantom body on a moving platform, the parameters of moving direction, breathing frequency and amplitude of the chest wall could be determined individually. The surface dose in the target region was calculated as the average of five TLD chips situated in five 1 mm deep holes with a

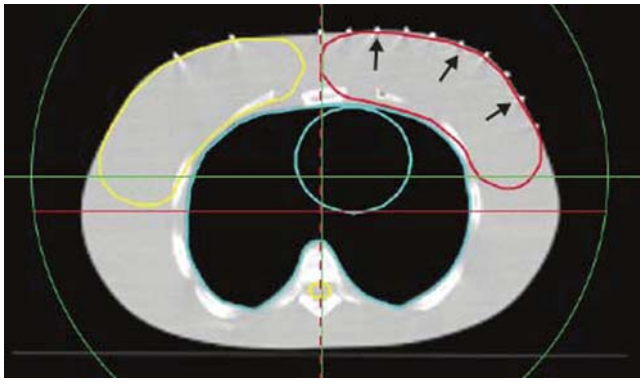

Figure 2. CT image of the static phantom. The black arrows mark the spots where the surface dose was measured. The PTV_{skin} is displayed in red, the contralateral breast in yellow, and the lungs and heart in blue. On the surface, the bright points are metal markers to make a precise TLD positioning and a plan reproduction possible.

Abbildung 2. CT-Bild des statischen Phantoms. Die schwarzen Pfeile markieren die Stellen, an denen die Oberflächendosis gemessen wurde. Das PTV_{skin} ist rot dargestellt, die kontralaterale Brust gelb und die Lungen und das Herz blau. Die hellen Punkte auf der Oberfläche entsprechen Metallmarkern, um eine präzise TLD-Positionierung sowie eine Vergleichbarkeit im Plan zu ermöglichen.

5-mm diameter. The angle of breathing motion was chosen as 45°. Breathing was simulated with a sinusoidal delta function with a frequency of ten, 15, and 20 breathing cycles per minute. Based on the data of Kinoshita et al. giving an average breathing motion of (mean ± standard deviation [SD]) of 1.3 ± 0,5 mm for lateral motion and 2.6 ± 1.4 mm for vertical (anterior-posterior) motion, two motion amplitudes were chosen for the measurements [6]. The first amplitude chosen was 1.4 mm in anterior-posterior and lateral direction and should resemble the typical human breathing motion range of shallow breathing. In addition, an abnormally large breathing motion of amplitude of 4.2 mm was simulated. For both amplitudes and all breathing frequencies, irradiation was performed with HT using a treatment plan of PTV_{skin} and PTV_{air}.

Patients

In the framework of quality assurance, surface doses in the target region of 17 patients treated with HT and seven patients treated with 3D-CRT were measured. In total, 33 fractions consisting of 179 single doses were measured for HT, while 14 fractions consisting of 70 single doses were measured for 3D-CRT. In 3D-CRT, five TLD envelopes were taped on the four quadrants and the nipple of the breast belonging to the target region of each patient. Depending on the clinical situation, the number of TLD envelopes in the target region per patient in HT varied between two and eleven envelopes due to scar tissue, in uni- or bilateral breast cancer. To make a direct comparison of the treatment methods, ten patients with unilateral breast cancer were compared concerning surface dose. Five of these patients

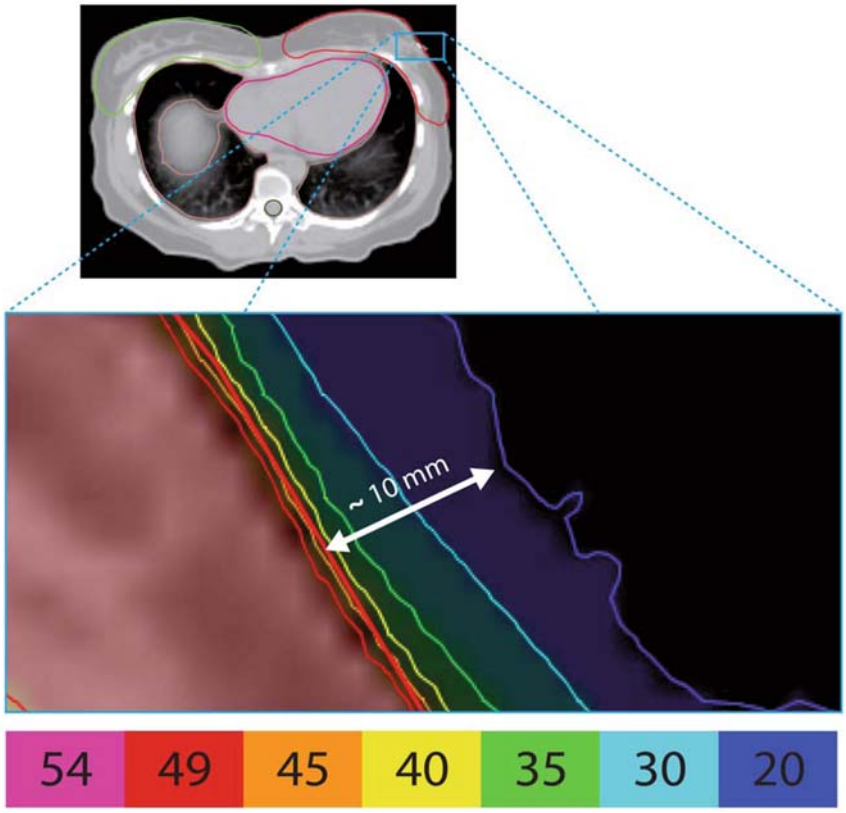

Figure 3. Typical treatment plan of a patient with left-sided breast cancer, comparable to the phantom plan PTVskin. Illustrated below is a zoomed-in cutout of the square in the surface region of the treatment plan with the corresponding isodose scale. The image shows the dose gradient, that can be found in the air layer above the PTV.

Abbildung 3. Typischer Bestrahlungsplan einer Patientin mit linksseitigem Mammakarzinom, der mit dem Plan PTVskin vergleichbar ist. Unten ist ein vergrößerter Ausschnitt des Quadrats im Oberflächenbereich des Bestrahlungsplans mit der dazugehörigen Isodosenskala dargestellt. Die Abbildung zeigt den Dosisgradienten, der in der Luftschicht oberhalb des PTV anzutreffen ist.

had an indication for an HT due to anatomic features, while the other five patients with a usual anatomy received 3D-CRT. All patients had in common, that the surface doses of two fractions each were measured with five TLD envelopes taped on the four quadrants and the nipple of the affected breast.

Results

Static Phantom

The measurements on the target region of the static phantom without mispositioning resulted in an average dose (mean ± SD) of 1.44 ± 0.04 Gy for the plan of PTV_{skin} and 1.48 ± 0.05 Gy for the plan of PTV_{air} in normal position (Figure 5). Mispositioning of the phantom to the right and posterior (into the PTV) in 2-, 5-, 8-, and 10-mm steps resulted in average relative deviations from the optimal dose of 7.2% [+4.6%; +9.7%] for PTV_{skin} and 1.8% [–3.2%; +4.7%] for PTV_{air}. Mispositioning with the same steps to the left and anterior had a much stronger impact on the surface doses. In the plan of PTV_{skin}, the values constantly decreased by positioning the phantom left and anterior to a minimum of 0.98 ± 0.11 Gy. This corresponds to relative deviations from the optimal dose in the range of –8.3% for the 2-mm to –31.9% for the 10-mm mispositioning. With values increasing up to 2.00 ± 0.17 Gy, the plan of PTV_{air} showed a strong increase of dose for the same mispositioning with relative deviations from the dose in normal position in the range of +14.2% for the 2-mm to +35.2% for the 10-mm mispositioning (Figure 5). The surface doses indicated for these specific points in the planning software were on average 10.6% higher than the measured values.

Dynamic Phantom

The results of the dynamic phantom are summarized in Table 1. The maximal relative surface dose deviations measured were between 0.8% and 3.8%. The highest deviations could be observed for the larger breathing amplitudes and the higher breathing frequencies. There was a negligible difference between the relative dose deviations of the plans of PTV_{skin} and PTV_{air}, indicating slightly higher deviations for the plan of PTV_{air}. In every measurement, a decrease of dose could be observed, when the phantom was moved. Also in this setup, the measured values were smaller than the calculated values of surface doses in the plan (on average 17.0%).

Patients

The average measured surface doses on the patients were (mean ± SD) 1.65 ± 0.13 Gy for HT and 1.42 ± 0.11 Gy for 3D-CRT (Figure 6). The 95% confidence intervals were [1.64; 1.67] Gy for HT and [1.39; 1.44] Gy for 3D-CRT. The Wilcoxon U-test showed a significantly higher surface dose for HT than for 3D-CRT with $p < 0.001$. Concerning HT, 21 of the 179 measured single doses were higher than the prescribed 1.8 Gy. The comparison of the average surface dose between five patients treated with HT and five patients treated with 3D-CRT with two fractions each is illustrated in Figure 7. The results are given as the average dose ± SD calculated with the five single doses from the five TLD envelopes in the target region. For the five HT patients, the average surface doses ranged from 1.59 ± 0.09 to 1.85 ± 0.14 Gy. The average surface

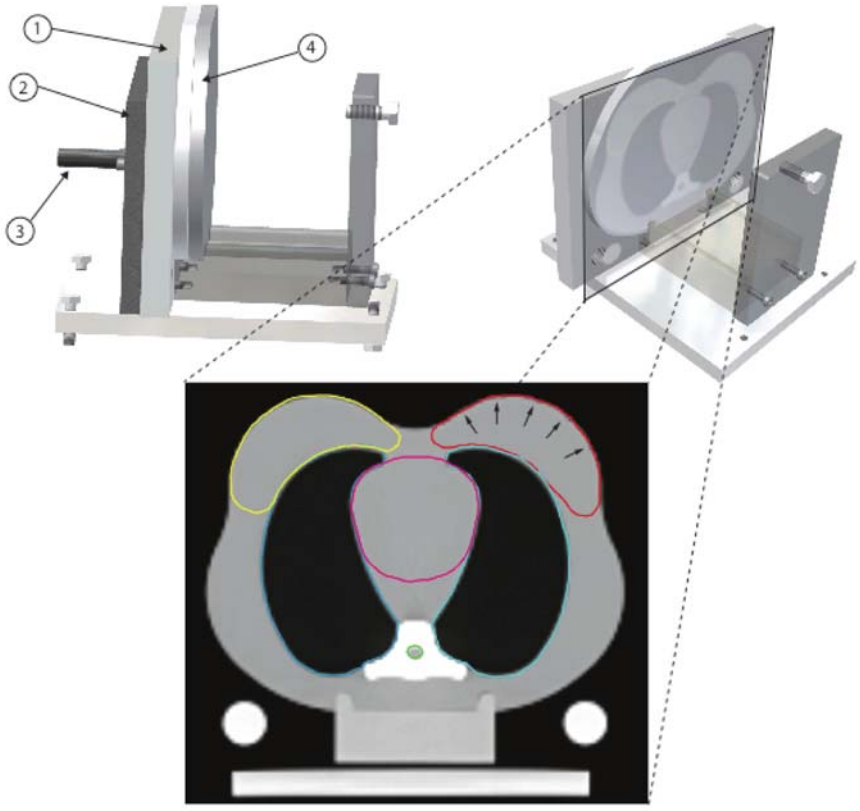

Figure 4. Dynamic phantom. Top: 1: phantom slice fastening; 2: electric motor fastening and bearing for 45° movement; 3: electric motor; 4: single phantom slice. Bottom: extract of one single phantom slice of the top right picture illustrated as a CT image with marked PTVskin (red) and organs at risk. To make the visualization easier, only one of the eleven slices of the phantom body was illustrated on this picture. The black arrows mark the points of measurement of the TLD chips.

Abbildung 4: Dynamisches Phantom. Oben: 1: Phantomscheibenhalterung; 2: Elektromotorhalterung und Lager für eine Bewegung von 45°; 3: Elektromotor; 4: einzelne Phantomscheibe. Unten: Auszug einer einzigen Phantomscheibe des Bilds oben rechts, dargestellt als CT-Bild mit markiertem PTVskin (rot) und Risikoorganen. Um die Visualisierung zu vereinfachen, wurde nur eine der elf Phantomscheiben des Phantomkörpers in diesem Bild dargestellt. Die schwarzen Pfeile markieren die Messpunkte der TLD-Chips.

doses in 3D-CRT ranged from 1.32 ± 0.07 to 1.47 ± 0.10 Gy. The maximal dose differences observed between two fractions of one patient were 0.09 Gy for HT and 0.07 Gy for 3D-CRT, respectively. The comparison of 52 measured single doses with those in the plan showed higher doses in the plan with an average dose increase of 6.1% of the measured value.

Discussion

The results of this study showed homogeneous and reproducible surface doses in the treatment of breast cancer with HT.

Several authors worked already on issues concerning surface dose in HT and found results indicating either significant or insignificant impact of the aforementioned factors on the surface dose [3, 12, 13, 22]. Mutic & Low, for example, measured the surface doses of HT with TLD on a water-equivalent phantom and showed that the HT planning system overestimates the surface dose of target volumes, especially when they are located close to the surface [12]. Ramsey et al. analyzed the surface dose of HT with TLD for target volumes located between 5 and 0 mm away from the surface on a RANDO head phantom [13]. They found that the deviation of the doses calculated by the tomotherapy planning software from the measured doses had an average value of +8.9% ± 3.2%. This data corresponds quite well to the average dose increase on the plan doses found in this study, being between +6.1% for the patients and + 17.0% for the dynamic phantom. Tournel et al. analyzed the dosimetric influence on the surface dose of a 5-mm mispositioning toward air and toward tissue with TLD and Kodak EDR2 film measurements on a static phantom [22]. They observed differences in the surface dose between –2.8% and +9% as compared to the dose in normal position. Ding et al. investigated the effect of the respiratory cycle and radiation beam-on timing on the dose distribution in free-breathing dynamic breast IMRT. Their results showed that the respiratory cycle period and radiation beam-on timing presented limited impact on the target dose coverage and slightly increased the target dose heterogeneity [3]. These results correspond well to the results of this study.

The latest results obtained by Moeckly et al. showed dose deviations of the prescribed dose of > 5% in a band of 10 mm in the apex region of the PTV, using a phantom with a simulated sinusoidal breathing amplitude of 5 mm [11]. The observed surface dose deviations due to constant sinusoidal breathing motion in this study, however, were < 5%.

Our present study investigates not only the dose gradients and dosimetric effect of movement on the surface dose, it also analyzes the effect of target volume definition within or out of skin level in both experimental phantom and clinical patient setup.

The results of the measurements on the static phantom indicate that there was only a limited effect on the surface dose, when the surface of the PTV was located into the original PTV definition in both plans. The mispositioning into the air showed large changes in surface doses. Although these extreme mispositionings are unlikely to happen in clinical routine, the

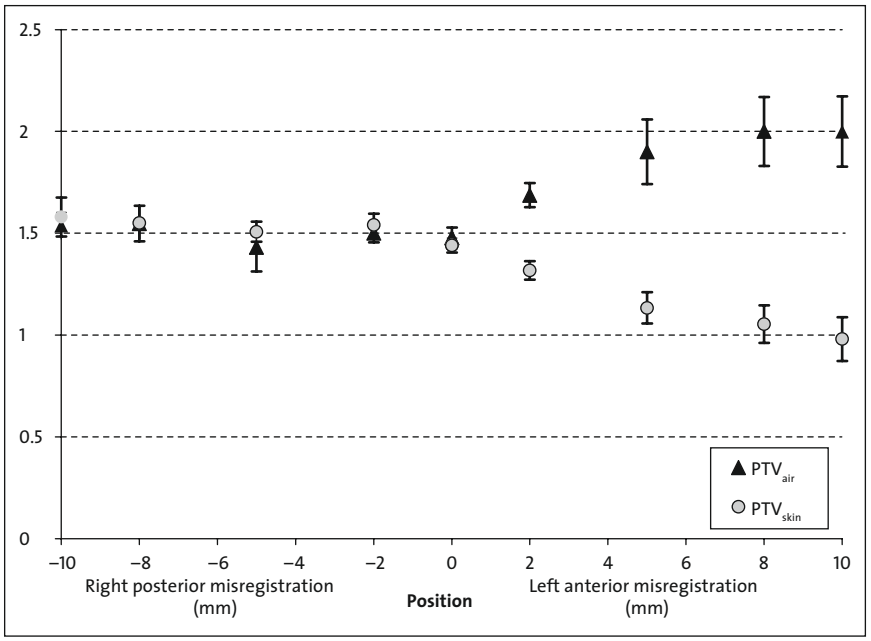

Figure 5. Static phantom misregistration. The triangles and circles reflect the average measured surface dose (n = 3) on a distinct position with a distinct plan. Position o reflects the "normal" position at treatment planning. The bars correspond to ± one standard deviation from the average dose measured.

Abbildung 5. Statisches Phantom, Fehlpositionierung. Die Dreiecke und Kreise geben den gemessenen Dosismittelwert (n = 3) bei einer bestimmten Position mit einem bestimmten Plan wieder. Position o entspricht der „Normalposition" bei Bestrahlungsplanung. Die Balken entsprechen ± einer Standardabweichung vom gemessenen Dosismittelwert.

Table 1. Dynamic phantom measurements. "Range" is the total breathing motion in the anterior-posterior and lateral directions. The values correspond to the average dose (n = 5) ± standard deviation.

Tabelle 1. Messungen am dynamischen Phantom. „Range" ist die absolute Atembewegung in anterior-posterioren und lateralen Richtungen. Die Werte entsprechen dem Dosismittelwert (n = 5) ± einer Standardabweichung.

Range	4.2 mm PTV_{skin} (Gy)	4.2mm PTV_{air} (Gy)	1.4mm PTV_{skin} (Gy)	1.4mm PTV_{air} (Gy)
Frequency				
• No movement	1.45 ± 0.09	1.48 ± 0.12	1.45 ± 0.09	1.48 ± 0.12
• 10/min	1.43 ± 0.08	1.44 ± 0.11	1.45 ± 0.09	1.45 ± 0.11
• 15/min	1.41 ± 0.06	1.43 ± 0.14	1.45 ± 0.08	1.47 ± 0.12
• 20/min	1.39 ± 0.07	1.43 ± 0.13	1.44 ± 0.09	1.47 ± 0.11
Maximal deviation	3.8%	3.5%	0.8%	1.9%

strong gradients should be considered especially concerning overdosage and hot spots when using a plan like PTV_{air}. Even a small mispositioning like the 2/2-mm step or a changing surface anatomy in this range which can vary day by day was enough to lead to a dose increase of 14.2% when using a plan like PTV_{air} compared to a decrease of 8.3% for PTV_{skin}. In the dynamic phantom setup, only small surface dose deviations could be observed in all measurements. In every measurement, a decrease of dose could be observed, when the phantom was moved. With a maximum of 3.8%, the deviations stayed well below the 5% measurement uncertainty of the TLDs [14]. Although the dose deviations of the plan PTV_{air} were almost the same as those of the plan PTV_{skin}, the problems of overdosage remain, due to misregistration error or a changing surface anatomy in the anterior direction of the PTV. In this setup no randomness of frequency and amplitude was integrated, so the dose error is expected to be smaller than for an in vivo random breathing condition. In this case, the results should be an approach to show the effects of a vertical and lateral motion of a typical patient with regular shallow breathing patterns on the surface dose. The dose effects of longitudinal breathing were not measured, as actual research found only small dose deviations for the typical breathing motion patterns [8]. The results of the patients showed a homogeneous dose distribution for both HT and 3D-CRT, with discrete advantages for the latter. As to average surface doses, a highly significant ($p < 0.001$) difference between HT and 3D-CRT could be observed. HT turned out to be the superior method for reaching the prescribed dose at the PTV's surface at the price of a slightly higher dose heterogeneity expressed by a higher SD of the measured values. With doses in the range of [1.81; 2.07] Gy, 21 of the 179 measured single doses were higher than the prescribed 1.8 Gy. The comparison of the five patients treated with different methods, however, indicated that overdosage problems seemed to occur more likely on single patients. It also showed slightly higher dose discrepancies between two fractions for HT. Considering the fact, that the maximal skin toxicity observed in all HT patients amounted to grade 1 (CTC [Common Toxicity Criteria]), the problem of overdosage of the surface in HT seemed to be in an acceptable range.

Conclusion

HT enables a homogeneous and reproducible surface dose with small dose deviations in the treatment of breast cancer. HT is a feasible method to treat breast cancer under free shal-

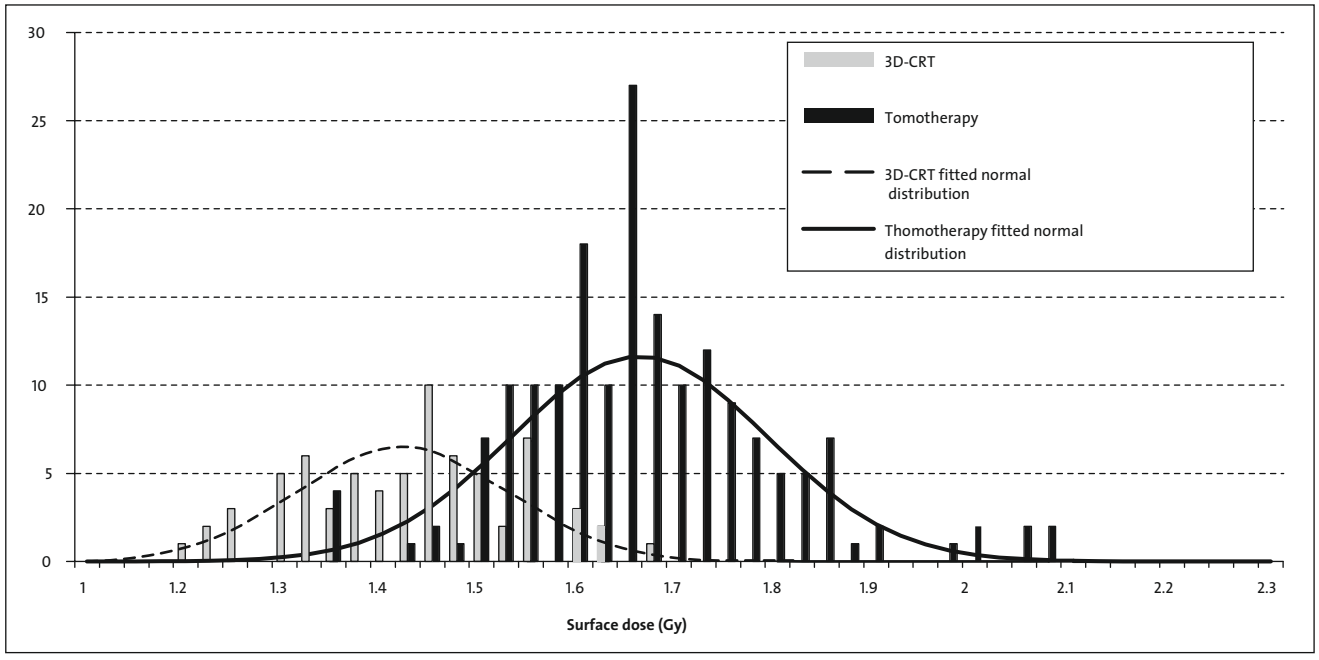

Figure 6. Patient surface dose measurements. Frequencies of the measured single doses on the surface in the target region for HT (n = 179) and 3D-CRT (n = 70). The curves are fitted normal distributions to ease the visual comparison and interpretation.

Abbildung 6. Oberflächendosismessungen bei Patientinnen. Häufigkeiten der gemessenen Einzeldosen auf der Oberfläche im Zielbereich bei HT (n = 179) und 3D-CRT (n = 70). Die Kurven sind angepasste Normalverteilungen, um den visuellen Vergleich und die Interpretation der Graphik zu vereinfachen.

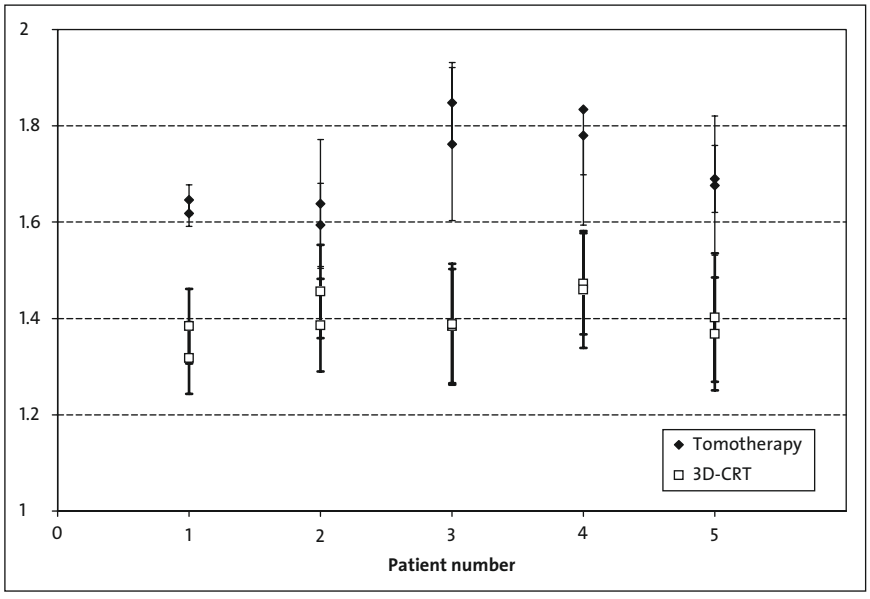

Figure 7. Comparison of surface doses of HT and 3D-CRT for five patients each. The two diamonds/squares correspond to the average surface dose (n = 5) of one fraction with HT/3D-CRT. The bars correspond to ± one standard deviation of the average dose in each direction.

Abbildung 7. Vergleich von Oberflächendosen bei HT und 3D-CRT von jeweils fünf Patientinnen. Die zwei Rauten/Quadrate entsprechen den mittleren Oberflächendosen (n = 5) einer Fraktion mit HT/3D-CRT. Die Balken entsprechen ± einer Standardabweichung vom Dosismittelwert.

low breathing of the patient. Drawing the PTV's outer contour at the skin level seems to be favorable compared to the additional inclusion of an air rim, as dose deviations due to misregistration errors are smaller. Despite breathing motion, HT enables significantly higher doses in the surface region than a three-dimensional conformal treatment.

Acknowledgments

This work was in part supported by the Deutsche Forschungsgemeinschaft (DFG) and a grant by the Medical Faculty of the University of Heidelberg (F.S.) and the Tumor Center Heidelberg/Mannheim.

References

1. Bauman G, Yartsev S, Rodrigues G, et al. A prospective evaluation of helical tomotherapy. Int J Radiat Oncol Biol Phys 2007;68:632–41.
2. Dawson LA, Sharpe MB. Image-guided radiotherapy: rationale, benefits, and limitations. Lancet Oncol 2006;7:848–58.

3. Ding C, Li X, Huq MS, et al. The effect of respiratory cycle and radiation beam-on timing on the dose distribution of free-breathing breast treatment using dynamic IMRT. Med Phys 2007;34:3500–9.
4. Fiorino C, Dell'Oca I, Pierelli A, et al. Simultaneous integrated boost (SIB) for nasopharynx cancer with helical tomotherapy. A planning study. Strahlenther Onkol 2007;183:497–505.
5. Kanagaki B, Read PW, Molloy JA, et al. A motion phantom study on helical tomotherapy: the dosimetric impacts of delivery technique and motion. Phys Med Biol 2007;52:243–55.
6. Kinoshita R, Shimizu S, Taguchi H, et al. Three-dimensional intrafractional motion of breast during tangential breast irradiation monitored with high-sampling frequency using a real-time tumor-tracking radiotherapy system. Int J Radiat Oncol Biol Phys 2008;70:931–4.
7. Kissick MW, Fenwick J, James JA, et al. The helical tomotherapy thread effect. Med Phys 2005;32:1414–23.
8. Kissick MW, Flynn RT, Westerly DC, et al. On the impact of longitudinal breathing motion randomness for tomotherapy delivery. Phys Med Biol 2008;53:4855–73.
9. Mackie TR, Balog J, Ruchala K, et al. Tomotherapy. Semin Radiat Oncol 1999;9:108–17.
10. Mackie TR, Holmes T, Swerdloff S, et al. Tomotherapy: a new concept for the delivery of dynamic conformal radiotherapy. Med Phys 1993;20:1709–19.
11. Moeckly SR, Lamba M, Elson HR. Respiratory motion effects on whole breast helical tomotherapy. Med Phys 2008;35:1464–75.
12. Mutic S, Low DA. Superficial doses from serial tomotherapy delivery. Med Phys 2000;27:163–5.
13. Ramsey CR, Seibert RM, Robison B, et al. Helical tomotherapy superficial dose measurements. Med Phys 2007;34:3286–93.
14. Robertson MA. Characteristics of TLD. In: Robertson MA, ed. Identification and reduction of errors in thermoluminescence dosimetry systems. Weybridge: Pittman, 1981:6–10.
15. Rochet N, Sterzing F, Jensen A, et al. Helical tomotherapy as a new treatment technique for whole abdominal irradiation. Strahlenther Onkol 2008;184:145–9.
16. Ruchala KJ, Olivera GH, Schloesser EA, et al. Megavoltage CT on a tomotherapy system. Phys Med Biol 1999;44:2597–621.
17. Sterzing F, Herfarth K, Debus J. IGRT with helical tomotherapy – effort and benefit in clinical routine. Strahlenther Onkol 2007;183:Special Issue 2: 35–7.
18. Sterzing F, Schubert K, Sroka-Perez G, et al. Helical tomotherapy. Experiences of the first 150 patients in Heidelberg. Strahlenther Onkol 2008;184: 8–14.
19. Thilmann C, Sroka-Perez G, Krempien R, et al. Inversely planned intensity modulated radiotherapy of the breast including the internal mammary chain: a plan comparison study. Technol Cancer Res Treat 2004;3: 69–75.
20. Thilmann C, Zabel A, Milker-Zabel S, et al. Number and orientation of beams in inversely planned intensity-modulated radiotherapy of the female breast and the parasternal lymph nodes. Am J Clin Oncol 2003;26:e136–43.
21. Thilmann C, Zabel A, Nill S, et al. Intensity-modulated radiotherapy of the female breast. Med Dosim 2002;27:79–90.
22. Tournel K, Verellen D, Duchateau M, et al. An assessment of the use of skin flashes in helical tomotherapy using phantom and in-vivo dosimetry. Radiother Oncol 2007;84:34–9.
23. Welsh JS, Patel RR, Ritter MA, et al. Helical tomotherapy: an innovative technology and approach to radiation therapy. Technol Cancer Res Treat 2002;1:311–6.
24. Yu CX, Jaffray DA, Wong JW. The effects of intra-fraction organ motion on the delivery of dynamic intensity modulation. Phys Med Biol 1998;43: 91–104.

Address for Correspondence
Dr. Florian Sterzing
Department of Radiation Oncology
University of Heidelberg
Im Neuenheimer Feld 400
69120 Heidelberg
Germany
Phone (+49/6221) 56-8202, Fax -5353
e-mail: florian.sterzing@med.uni-heidelberg.de